Evaluation of the performance of a Navier-Stokes and a viscous-inviscid interaction solver in trailing edge flap simulations

John Prospathopoulos, jprosp@fluid.mech.ntua.gr
Giorgos Papadakis, papis@fluid.mech.ntua.gr
Alexis Theofilopoulos, atheofi@yahoo.gr
Theofanis Tsiantas, th.tsiantas.mech.ntua@gmail.com
Vasilis Riziotis, vasilis@fluid.mech.ntua.gr
Spyros Voutsinas, spyros@fluid.mech.ntua.gr

National Technical University of Athens, 9 Heroon Polytechniou, 15780, Zografou, Athens, Greece

Abstract:

Trailing edge flap is one of the most common flow control devices aiming at reducing the loads on the wind turbine blades. From the modelling point of view the dynamic character of flap introduces challenges, including unsteady flow phenomena and moving/deformable meshes. In the present paper airfoils with flapping trailing edge are simulated using two different computational tools, one viscous-inviscid interaction code and one compressible Navier-Stokes code. The predictions of the codes for static and dynamic flap situations are compared to the existing measurements. In the static flap cases, predictions of both models were satisfactory in the linear region. In free transition the better predictions of the drag coefficient by the viscous-inviscid interaction code are attributed to the different transition model. In the dynamic flap cases, combined with a harmonic pitching motion of the airfoil, part of the differences emanates from the fact that the actual (measured) flap angle deviates from the nominal one as reported by the experimenters.

Keywords: Trailing edge flap simulation, viscous-inviscid interaction, CFD, transition models.

1 Introduction

Lifetime of large wind turbines depends on the aerodynamic and structural loads experienced during operation. Most of these loads exhibit periodic variation in multiples of the rotational frequency. To minimize these loads, control systems should be able to reduce the fluctuations of the aerodynamic loads or add damping to the structural modes. On the other hand the aerodynamic performance of the airfoils along the blade span should be maximized. Flow control devices, such as trailing edge (TE) flaps or vortex generators, aim at mitigating the fatigue loads and improving the aerodynamic performance of an airfoil. In the framework of AVATAR.EU FP7 project the effect of flow control devices on large wind turbine blades is investigated.

In the present paper, trailing edge flap is investigated using simulations by two in-house computational tools developed at NTUA. The first is the Foil1w viscous-inviscid interaction code [1] and the second is the MaPFlow compressible Navier-Stokes solver [2]. Two different cases with available experimental data were chosen: The first refers to static TE flap for which steady state simulations are performed. For that case, the experimental data are taken from the measurements of the TL190-82 airfoil performed in the course of the European UPWIND project at the wind tunnel of the Institute of Aerodynamics and Gas Dynamics (IAG), University of Stuttgart [3]. The second case refers to dynamic TE flap for which unsteady state simulations are performed. In that case the experimental data are taken from measurements on NACA0012 carried out by Krzysiak and Narkiewicz in the trisonic N-3 wind tunnel located at the Institute of Aviation Warsaw, Poland [4].

2 Numerical models

Foil1w: Foil1w is a viscous-inviscid interaction code developed at NTUA. The potential flow part is simulated by singularity distributions along the airfoil geometry and the wake. The wake is

represented by vortex particles which are allowed to freely move with the local flow velocity.

The viscous flow solution is obtained by solving the unsteady integral boundary layer equations defined by Drela [5] with unknowns the displacement thickness, the momentum thickness and the amplification factor (laminar part) or the shear stress coefficient (turbulent part) through which C_D is determined. The viscous-inviscid coupling is achieved through a transpiration velocity distribution along the airfoil surface that represents the mass flow difference over the boundary layer height between the real viscous flow and the equivalent inviscid flow.

The boundary layer equations are discretized using finite differences and the final set of the non-linear equations are solved simultaneously using the Newton-Raphson algorithm. The boundary layer solution is supplemented by a transition prediction model based on the e^N spatial amplification theory [6] and by a dissipation closure equation for the maximum shear stress coefficient over the turbulent part.

MaPFlow: MaPFlow is a multi-block MPI enabled compressible solver equipped with preconditioning in regions of low Mach flow [7]. The discretization scheme is cell centered and makes use of the Roe approximate Riemann solver for the convective fluxes. In space the scheme is 2nd order accurate defined for unstructured grids and applies the Venkatakrishnan's limiter [8]. Also in time the scheme is second order and implicit introducing dual time stepping for facilitating convergence. The solver is equipped with the Spalart-Allmaras (SA) and the k-w SST eddy viscosity turbulence models.

Regarding transition, the correlation γ-Re_θ model of Menter [9] has been implemented. The γ-Re_θ is a two transport equation model for the intermittency and the momentum thickness Reynolds number. It utilizes local variables easily computed in each cell and does not need boundary layer definition and parameters.

3 Simulation of Trailing Edge flap

3.1 Static TE flap cases

For the TL190-82 airfoil (Figure 1), static TE flap deflections from -10 to 10 degree are simulated in clean and tripped conditions at a Reynolds number of $2.5 \cdot 10^6$. MaPFlow used an O-type mesh of 150000 cells generated by ICEM CFD. The non-dimensional distance of the first node from the wall is less or equal to 10^{-5}. Foil1w can use only sharp airfoil profiles, so the original blunt airfoil profile is made sharp by modifying the aft of the original shape and discretized with a number of 100 panels. Clean conditions are simulated with free transition modeling, whereas tripped conditions are simulated with fully turbulent and fixed transition modeling by MaPFlow and Foil respectively.

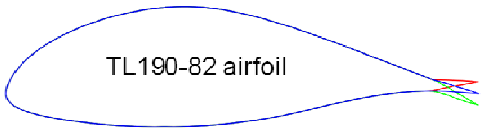

Figure 1: Articulated TE flap for the TL190-82 airfoil

The predictions of the lift and drag coefficients are compared with the measurements in Figures 2,3. In clean conditions, both models predict lift well in the linear region. The fact that Foil1w predicts drag better than MaPFlow suggests that the e^N transition model identifies the transition locations more accurately than the γ-$Re\theta$ model. Differences among predictions appear at higher AoAs and are more pronounced in the post-stall region. In general, stall is predicted at higher AoAs compared to the measurements. Tripping appears to have a drastic effect on the measurements by shifting stall to lower AoA. This effect is less pronounced in the predictions which present larger deviations from the measurements compared to clean conditions.

In tripped conditions, the predictions of MaPFlow are closer to the measurements, in terms of both lift and drag. As expected the more advanced CFD model predicts friction more accurately than the boundary layer model in turbulent flow conditions.

3.2 Dynamic TE flap cases

Dynamic TE flap cases of the NACA0012 airfoil refer to a Reynolds number of $1.63\ 10^6$. A rigid trailing edge flap is implemented with a length 20% of the airfoil chord. The reduced frequency of the airfoil pitching motion is $k_A = 0.021$, while the flap oscillation has a double frequency, $k_F = 0.042$. The angle of attack (pitch angle) and the flap deflection are governed by the equations

$$a = a_m + \Delta\alpha \ \sin(2k_A t) \ , \qquad (1)$$

$$\beta = \beta_m + \Delta\beta \ \sin(2k_F t - \varphi) \qquad (2)$$

where α_m and β_m are the mean values of the angle of attack and flap deflection, $\Delta\alpha$ and $\Delta\beta$ are the amplitudes of the airfoil and flap harmonic movement respectively and φ is the phase shift between the airfoil and the flap angle.

In all simulated cases $\alpha_m = 4^o$, $\Delta\alpha = 6$, $\beta_m = 0^o$ and $\Delta\beta = 5^o$ is considered while the effect of varying φ on aerodynamic loads is investigated. It is noted that positive pitching angle is the one that leads to nose up motion of the airfoil (increasing angles of attack) while positive flap deflection angle is the one obtained when the flap moves downwards.

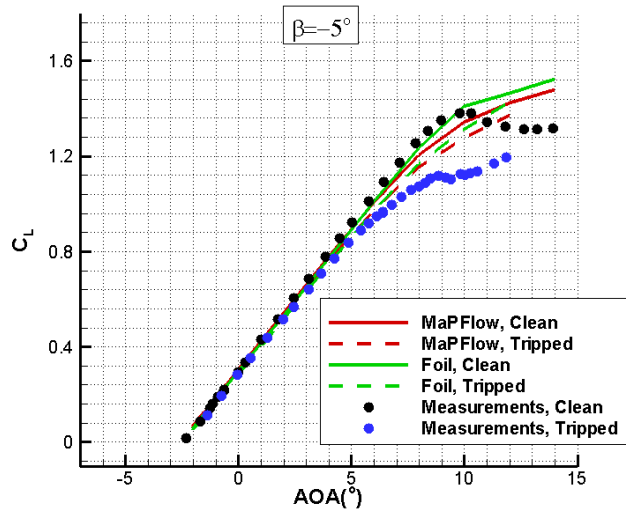

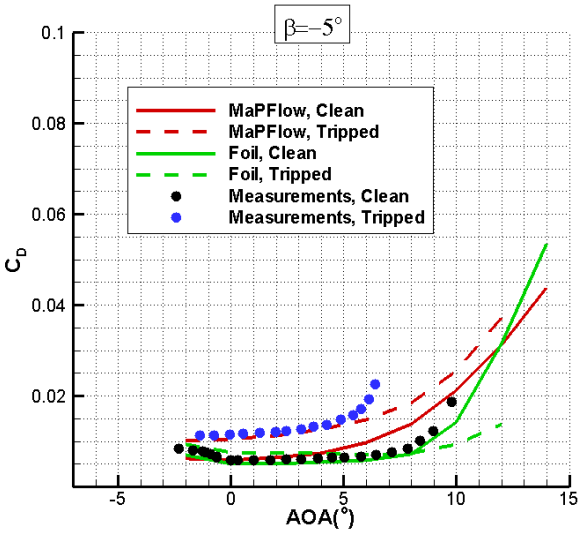

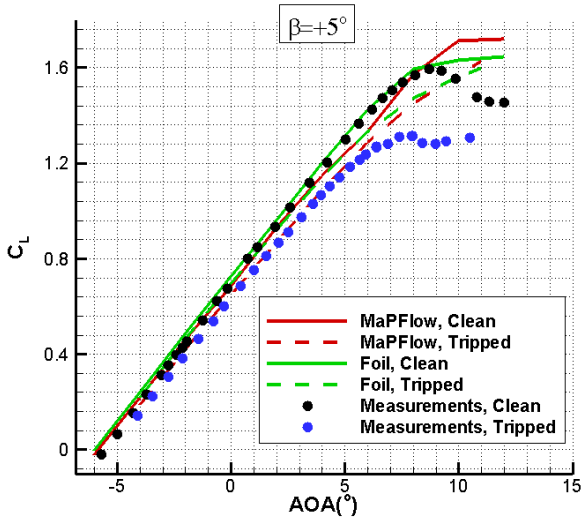

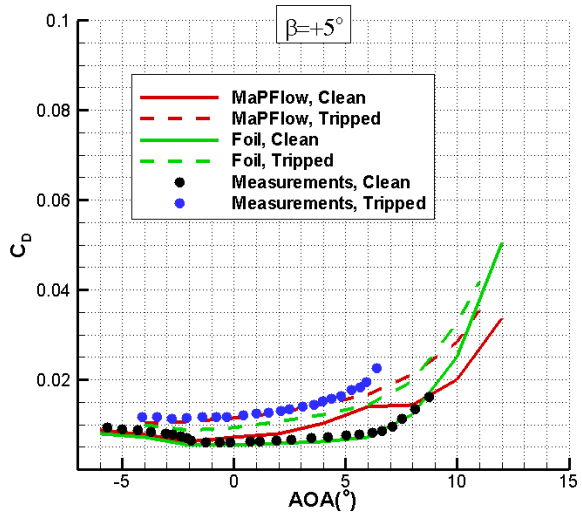

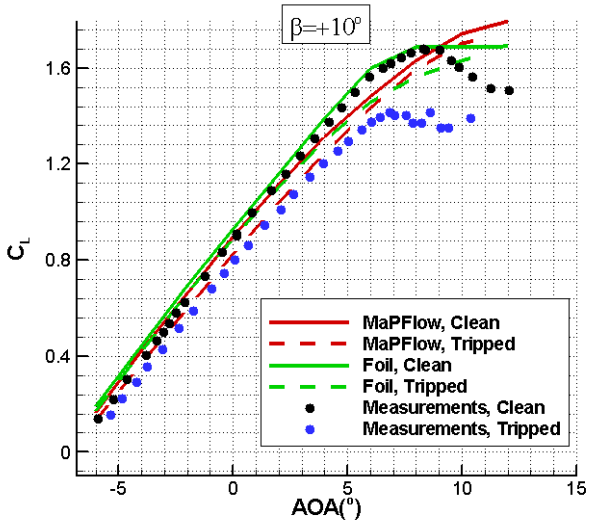

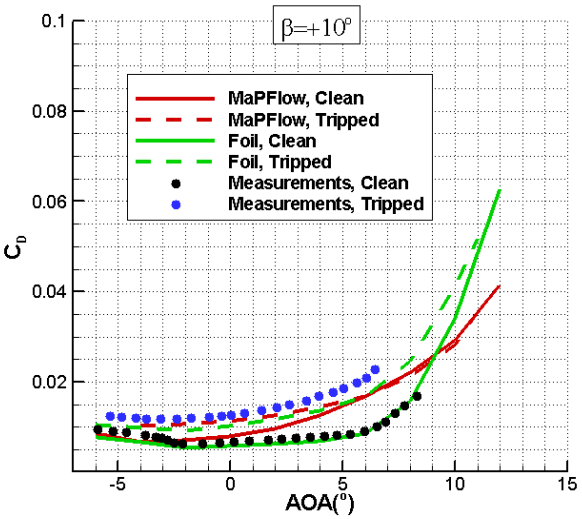

Figure 2: C_L polars for TE static flap, TL190-82 airfoil, Re=2.5·10^6. Flap angle takes the values -5^o, +5^o and +10^o. Clean conditions correspond to free transition and tripped conditions correspond to fixed transition

Figure 3: C_D polars for TE static flap, TL190-82 airfoil, Re=2.5·10^6. Flap angle takes the values -5^o, +5^o and +10^o.. Clean conditions correspond to free transition and tripped conditions correspond to fixed transition

MaPFlow uses a C-type mesh of 88000 cells generated by ICEM CFD (Figure 4) and performs fully turbulent simulations. One flapping period is discretized using 720 time steps. The code runs initially for constants AoA= α_m and flap angle= β_m until a steady state solution is reached and then the harmonic variations of both angles are imposed. A periodic solution is achieved after 6 flapping periods. Foil1w considers fixed transition at 5% chord from the leading edge. One flapping period is discretized using 400 time steps and convergence is achieved again after 6 flapping periods.

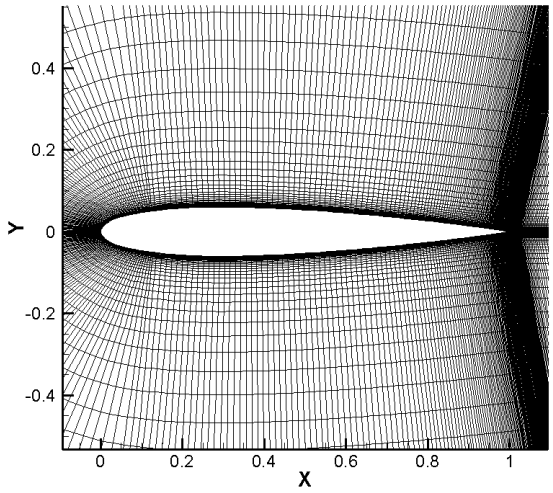

Figure 4: Computational mesh around the NACA0012 airfoil

The different test cases refer to different phase shifts between the airfoil pitching motion and the flap angle. Figure 5 shows the variation of the flap angle with the angle of attack for φ=148°, φ=206° and φ=298°. Measurements deviate from the nominal values provided by Equations (1),(2) possibly due to elastic deformations occurred during the experimental campaign or delay/errors in the response of the actuators controlling the motion of the airfoil and the flap. In order to fit the measured airfoil phase /flap relative motion, Nestor [10] suggested corrections to the phase shift from φ=148° to φ=135°, from φ=206° to φ=196° and from φ=298° to φ=280°. The double frequency of the flap movement results in the appearance of two loops, one corresponding to a whole flap cycle when AoA is positive and another one corresponding to a whole flap cycle when AoA is negative.

In order to estimate the effect of the phase shift correction, as suggested by Nestor, to the predictions, some initial simulations are performed with Foil1w. In Figure 6, the modified C_L, C_M loops for φ=148° are compared with those of φ=135° which is the corrected phase shift. Differences with measurements have been decreased suggesting that an even better correlation with the measured flap angle may result in a better and more fair comparison

.

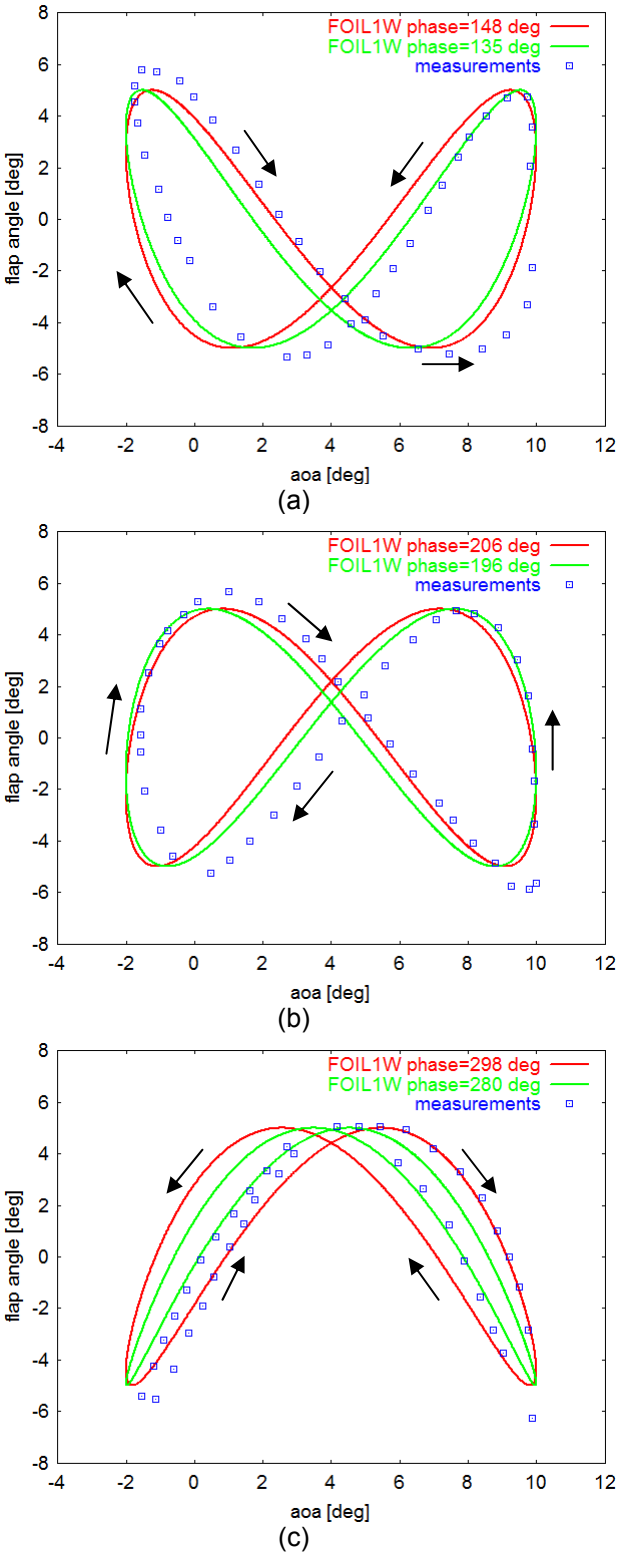

Figure 5: Theoretical and measured variation of the flap angle with the angle of attack (i.e. pitching angle) for (a) φ=148°, (b) φ=206° and (c) φ=298°. Nestor [12] suggested phase corrections from 148° to 135°, from 206° to 196° and from 298° to 280° in order to fit the measured airfoil / flap relative motion

For the comparison between predictions and measurements, the corrected phase shift is

adopted. In Figures 7,8, the predicted C_L, C_M loops are presented. The overall shape of the loops is reproduced by both models, however, lift is generally overpredicted and moment is underpredicted. Larger differences are observed at the positive AoAs and are responsible for the overestimation in the slope of the double loop (C_L-AoA diagrams, Figure 7). A part of these differences can be attributed to the deviation of the measured flap angles from the theoretical values or to the 3D effects related to the experiment, such as the creation of stall cells along the blade model.

For example, in Figure 5a, it can be observed that during the upstroke measured flap angles are lower than the nominal (positive AoA, negative flap), reducing the lift. A similar observation can be made in Figure 5b, where the measured values of the flap deflection are again more downwards than the theoretical used in the simulations, when the airfoil is in the downstroke phase (negative AOA, negative flap). Estimation of the 3D effect on the slope of the lift loops could be made by comparing predicted and measured lift polars at static TE flaps. However, no measurements have been reported for static TE flap.

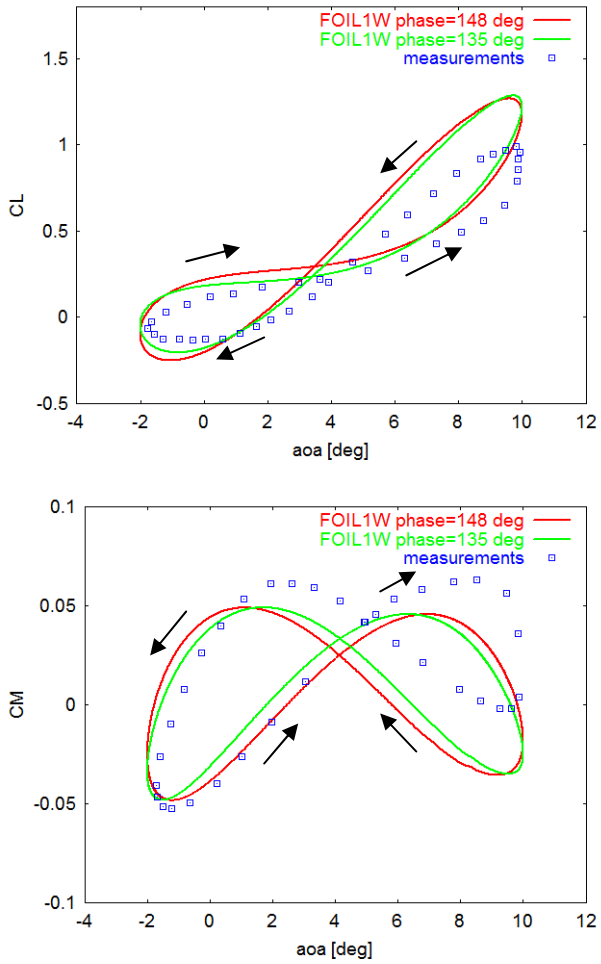

Figure 6: Modification in C_L, C_M coefficients predicted by Foil1w when the phase shift is corrected from 148° to 135°

It should be noted that Foil1w predictions are closer to the measurements compared to those of MaPFlow. One possible reason is that MaPFlow used fully turbulent simulation instead of fixed transition. On the other hand, there are no experimental data for drag, which is expected to be better predicted using the k-ω SST turbulence model implemented in MaPFlow.

4 Conclusions

Several static and dynamic TE articulated flap cases were simulated by two solvers, the MaPFlow CFD solver using the k-ω SST turbulence model, and the viscous-inviscid interaction Foil1w model using the e^N transition model. Regarding the static TE cases, numerical models give acceptable C_L errors in the linear region. In free transition cases, the e^N transition model showed a better behavior than the γ-Reθ transition model, probably because it predicts the transition locations more accurately. The location of the $C_{L,\,max}$ was not well reproduced by the numerical models. Therefore, in the post-stall region the predicted errors were almost doubled compared to those found in the linear region. In the tripped condition cases, drag was better predicted by the fully turbulent simulations of the CFD code using the k-ω SST model.

Regarding the dynamic TE flap cases (along with a harmonic movement of the airfoil), the measured flap angle deviated from the one obtained from the theoretical relationships to be used as input to the simulations. This is a first reason for the differences between predictions and measurements of the lift and moment coefficients. Although the correction suggested by Nestor partly improved the correlation with the experimental data, an even more accurate representation of the input flap angle must be sought. One way to do this is by approximating the flap angle variation by a Fourier series in which higher order harmonics are retained. A first attempt was made for the φ=206° case as shown in Figure 9. The flap representation is much closer to the measured one (six coefficients of the Fourier series are retained in this case), and the Foil1w C_L, C_M predictions have been considerably improved. C_L comes close to the measurements during the downstroke of the airfoil at positive flap angles, while C_M comes close to the measurements again during the downstroke of the airfoil but at negative flap angles. More simulations using both Foil1w and MaPflow codes must be performed to evaluate the effect of a more accurate flap angle representation on the predictions.

Another reason for the differences between predictions and measurements could be the 3D effects, such as the creation of stall cells along the blade model. Nevertheless, the comparison is encouraging because the shape of the lift and momentum variations was well reproduced and the

mean level was predicted satisfactorily in many cases.

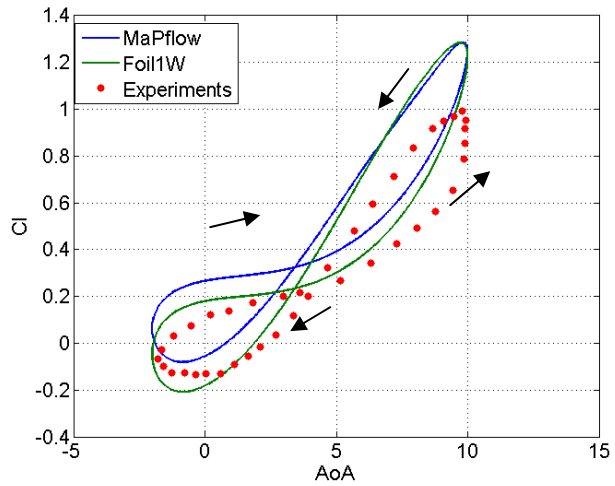

(a)

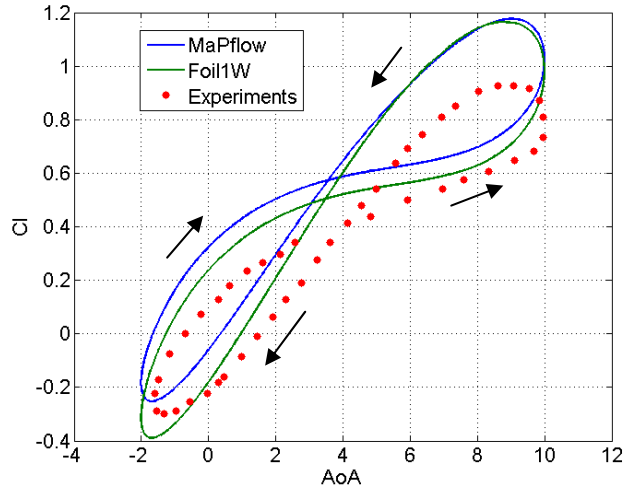

(b)

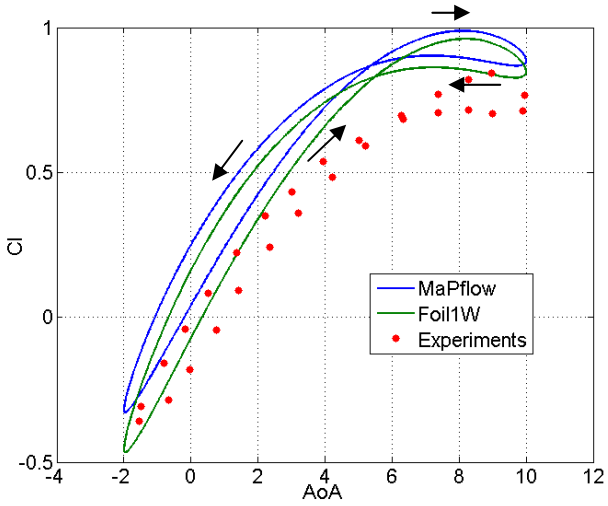

(c)

Figure 7: Comparison of predicted C_L coefficients with measurements. Phase shift is (a) 135°, (b) 196° and c) 280°

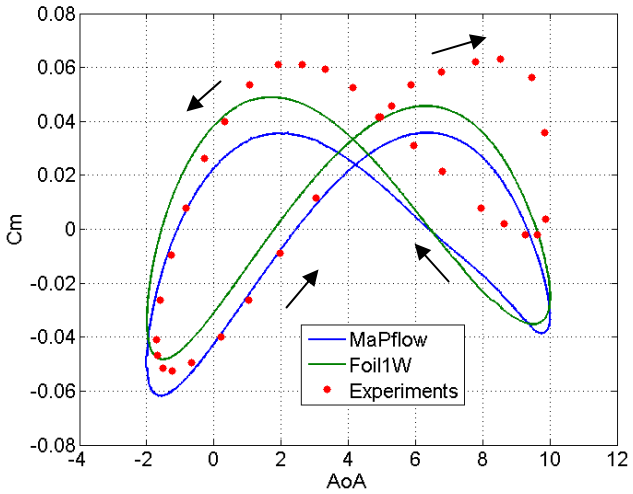

(a)

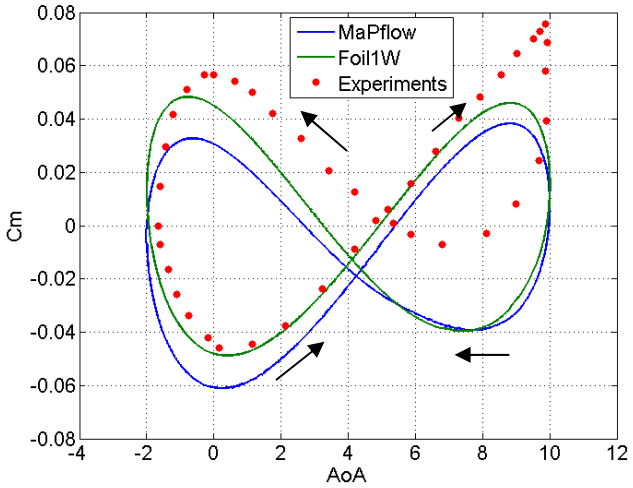

(b)

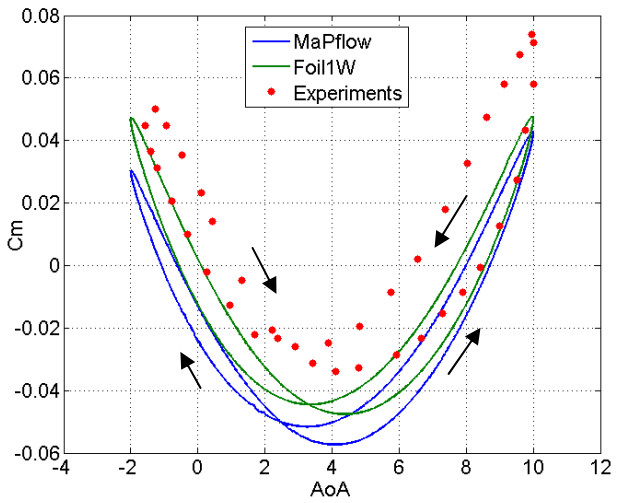

(c)

Figure 8: Comparison of predicted C_M coefficients with measurements. Phase shift is (a) 135°, (b) 196° and c) 280°

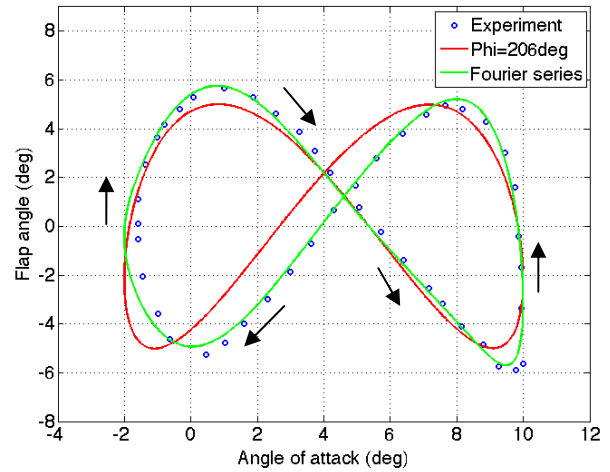

(a)

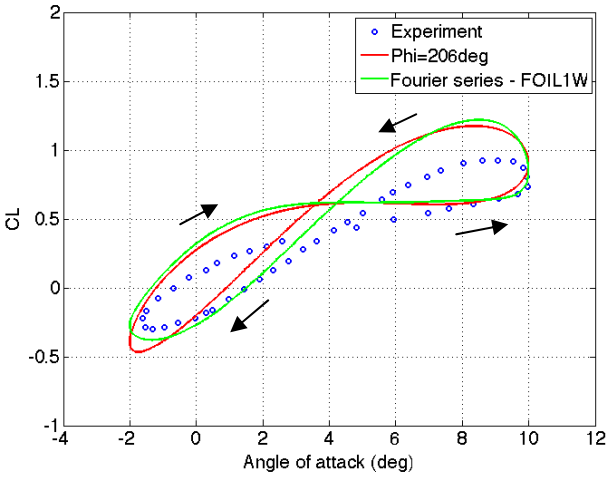

(b)

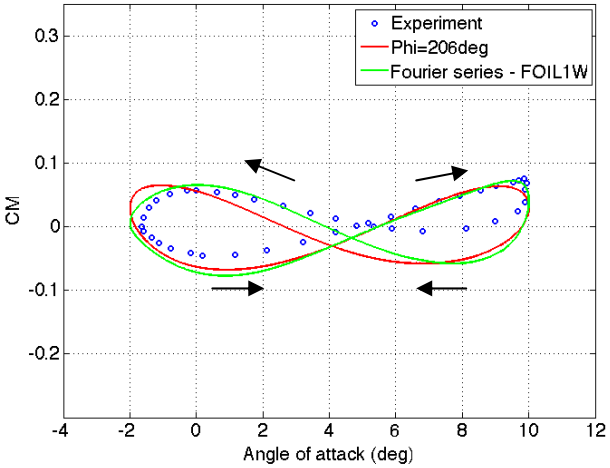

(c)

Figure 9: Representation of the flap angle variation using Fourier series and predicted C_L, C_M by Foil1w. Comparison with the predictions derived by the nominal flap angle variation: (a) Flap angle variation, (b) C_L and (c) C_M

Acknowledgment

The research leading to a part of these results has received funding from the European Community's Seventh Framework Programme under grant agreement No. 2013- 608396 (AVATAR.EU)

References

[1] Riziotis V.A. and Voutsinas S.G., 2008, "Dynamic stall modelling on airfoils based on strong viscous–inviscid interaction coupling", *International Journal for Numerical Methods in Fluids* 56 2 185-208

[2] Papadakis G. and Voutsinas S.G., 2014, "In view of accelerating CFD simulations through coupling with vortex particle approximations" in: *The Science of Making Torque from Wind Journal of Physics: Conference Series*, IOP Publishing Copenhagen pp. 012126

[3] Lutz T. and Wolf A., 2010, "Aerodynamic and acoustic design of wind turbine airfoils with trailing-edge flap" in Proceedings of DEWEK 2010, DEWI, Germany.

[4] Krzysiak, A. and Narkiewicz, N. "Aerodynamic loads on airfoil with trailingedge flap pitching with different frequencies". *Journal of aircraft*, 43:407-418, 2006

[5] Drela M, Giles M., "Viscous–inviscid analysis of transonic and low Reynolds number airfoils". *AIAA Journal* 1987; 25(10):1347–1355

[6] van Ingen JL., "A suggested semi-empirical method for the calculation of the boundary layer transition region". *Report VTH-74*, Department of Aerospace Engineering, Delft University of Technology, 1956.

[7] Papadakis G. and Voutsinas S.G, "In view of accelerating CFD simulations through coupling with vortex particle approximations", in: *The Science of Making Torque from Wind Journal of Physics: Conference Series*, IOP Publishing Copenhagen pp. 012126, 2014

[8] Venkatakrishnan V. "On the accuracy of limiters and convergence to steady state solutions", AIAA Paper 93-0880, 1993

[9] Robin B. Langtry, Florian R. Menter: "Correlation-Based Transition Modeling for Unstructured Parallelized Computational Fluid Dynamics Codes", AIAA Journal, Vol. 47, No. 12, December 2009..

[10] Nestor Ramos Garcia, "Unsteady Viscous-Inviscid Interaction Technique for Wind Turbine Airfoils", PhD Thesis, DTU Department of Mechanical Engineering, April 2011.